Mean-field theory of Coulomb blockade distribution for a disordered ensemble of quantum dots

Akashdeep Kamra
Department of Electrical Engineering, IIT - Kanpur, Uttar Pradesh - 208016, India

Praveen Pathak* and Vijay A. Singh
Homi Bhabha Centre for Science Education (TIFR), V. N. Purav Marg, Mankhurd, Mumbai-400088, India
(Received 12 July 2007; revised manuscript received 1 January 2008; published 3 March 2008)

Techniques for synthesizing quantum dots (QDs) result in an assembly in which a certain amount of disorder is inevitable. Experimental probes often record the collective properties of an assembly of QDs and not exclusively that of a single QD. On the other hand, theoretical calculations often limit themselves to an analysis of a single QD. In the present work we present a mean field theory for Coulomb blockade (CB) in an assembly of QDs. We consider two types of disorder: (i) Size disorder; e.g., QDs have a distribution of sizes which could be unimodal or bimodal in nature. (ii) Potential disorder with the confining potential assuming a variety of shapes depending on growth condition and external fields. We illustrate our methodology assuming a Gaussian or logarithm normal distribution in disorder in both size and potential. However, our theoretical framework can accommodate any experimentally provided distribution in disorder. To do this we rely on the scaling laws for CB (also termed as *Hubbard U*) obtained for an isolated QD. We observe that CB is partially suppressed by the disorder. This suppression is greater for bimodal distribution. Further, the distribution in U is a skewed Gaussian with enhanced broadening. We invoke the Lifshitz argument to analyze the bimodal case. We suggest how this distribution in CB can be experimentally studied.

DOI: 10.1103/PhysRevB.77.115302 PACS number(s): 73.23.Hk, 71.23.An, 73.21.La

I. INTRODUCTION

Quantum dots (QDs) are structures in which charge carriers are trapped in a nanometer size potential boundary. They consist of 10^3–10^6 atoms, with sizes in the range of 1–10 nm. Electronic levels in them are quantized and exhibit a shell structure. Thus they are also known as "artificial atoms."[1,2] They are of fundamental and technical interest for future electronic devices. An important achievement of today's technological drive towards smaller devices is the fabrication of the single-electron transistor which can be operated at room temperature.[3] QDs may also form the basis of a new generation of lasers.[4]

Arrays of QDs have been experimentally studied for some twenty years now.[5–11] Our aim is to understand Coulomb blockade (CB) for such an ensemble of QDs employing a minimal set of broad and plausible assumptions. As the name suggests, CB is the energy price paid on adding an electron to a QD. Classically, this price is $\approx e^2/C$, where e is electron charge and C is the capacitance of the QD. In many-body quantum mechanics, this "price" is given a name, namely *Hubbard U*. A QD constitutes a classic example of a mesoscopic system as mentioned by Tinkham.[12] Adding even one electron in a metallic QD which has a pool of about 10^5 electrons leads to observable effects.

Theoretical work on CB in a single quantum dot, both two and three dimensional, is more than a decade old. This work is carried out within an effective mass theory paradigm with many-body effects accounted for by the local density or local spin density approximation (EMT-LDA or EMT-LSDA).[13] Harmonic confinement of electrons is often employed. Systematic work with a variety of confinements (triangular, square, etc.) has also been carried out.[14] As mentioned above, work on quantum dot arrays has also been reported. The present work also deals with arrays. It considers spherical quantum dots with a variety of confinement potentials. It is reasonable to assume that such an array may have size dispersion as well as disorder in confinement. Our work addresses these issues.

In Sec. II we describe our model for a distribution of CB in a random array of three-dimensional quantum dots. We build up on earlier work on single quantum dots and discuss how to account for disorder in size and confinement in a mean field fashion. Our model includes a possible setup for the experimental verification of this analysis. In Sec. III we apply this model to the case of unimodal Gaussian and logarithm normal distribution in sizes of QDs. In Sec. IV we extend a similar analysis to an ensemble of QDs having bimodal distribution in size. Along with this we introduce the concept of a different kind of disorder related to the spatial arrangement of QDs. We invoke the Lifshitz argument[15] to analyze this disorder. The next section (Sec. V) considers disorder in confinement potential. Section VI constitutes the discussion. We also critique our work and suggest future directions.

II. MODEL

Extensive calculations on CB in a single three-dimensional QD were carried out by Pandey *et al.*[14] These calculations were done within the EMT-LDA and EMT-LSDA framework and took into account the Coulomb, exchange, and correlation effects. The Coulomb blockade (CB) was estimated by an effective *Hubbard U*. A scaling law for U was proposed which in the simplest case depends on the size R of the QD in the following fashion:[14]

$$U = \frac{C}{R^{\beta}}, \tag{1}$$

where the value of $\beta \in [0.33, 1]$ depends on the confinement potential. It was found that $\beta \approx 0.33$ when confinement is

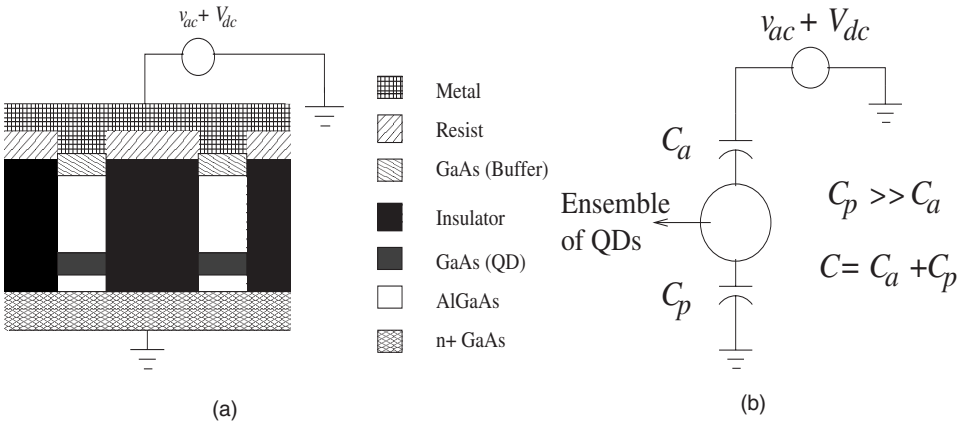

FIG. 1. (a) The sample under investigation. For simplicity we depict only two QDs. The passive lead consists of n^+ GaAs which is separated from GaAs (QD) by a thin insulating AlGaAs layer. A thicker AlGaAs insulating layer separates the QD from the active metallic lead. QDs are separated from each other by an insulating layer. (b) The electrical equivalent circuit for the sample under study.

quasitriangular, and β approaches 1 as confinement tends towards a quasisquare well.[14] It was also shown by Pandey *et al.*[14] that the popular case of harmonic confinement corresponds to $\beta \approx 0.5$ and not $\beta=1$ as is often assumed. It was further shown that U has a very weak dependence on the number of electrons (N) already present in the QD.

$$\beta(N) \sim N^{\eta}, \quad \eta \approx 0.05; \tag{2}$$

this implies that the results of our proposed model may hold up well for an arbitrary occupancy of the quantum dot.

We propose to understand CB in an assembly of QDs by combining the single dot result with two sister approaches: the one due to Kane[16] recently extended to the interpretation of photoluminescence spectra of porous silicon by Singh and George,[17] and the well-known Lifshitz argument.[15]

Let $P(U)$ be the distribution in U for a given distribution P_R in dot size. Then $P(U)$ is simply the convolution integral over P_R,

$$P(U) = \int_0^{\infty} \delta\left(U - \frac{C}{R^{\beta}}\right) P_R dR, \tag{3}$$

where we have used Eq. (1). Once the distribution in U is obtained we can calculate the energy U_p corresponding to peak in $P(U)$, the dispersion in U, and other related quantities.

We propose a setup for a possible experimental realization of $P(U)$. This setup is a modified version of the single electron capacitance spectroscopy (SECS) technique described by Ashoori.[2] A similar photoluminescence arrangement has also been described by Schmidt *et al.*[18] Consider the setup in which the QDs are located between two leads separated from the QDs by two insulating layers. One of the insulating layers is thick enough (~100 nm) not to allow any tunneling through it while the other one (~10 nm) is transparent to electrons. We call the lead corresponding to transparent tunnel junction the "passive" lead and the other one is called "active" lead. Figure 1(a) depicts a possible experimental realization. Figure 1(b) is the electrical equivalent circuit for the sample under study.

The passive lead is put to ground while a superposition of a positive dc (V_{dc}) and an ac ($v_{ac} \sin \omega t$) voltage is applied to the active lead. Here we define V such that

$$V = v_{ac} \sin \omega t + V_{dc}. \tag{4}$$

The amplitude of ac voltage (v_{ac}) is chosen so that it is slightly greater than kT and much smaller than V_{dc} ($kT < v_{ac} \ll V_{dc}$).

For the calculation of the response to the applied voltage, consider the charge due to electrons on the sample under study at the instant depicted in the energy level diagram (Fig. 2).

$$q = -2e \int_{-\infty}^{\infty} f(E + eV) D\left(E + e\frac{C_a}{C}V\right) dE, \tag{5}$$

where $f(E)$ is the Fermi function, $D(E)$ is the density of states (DOS) of the sample, C_a is the capacitance between the sample and the active lead, and C is the total capacitance associated with the sample. Note that $C=C_a+C_p$, here C_p is the capacitance between the sample and passive lead [see Fig. 1(b)]. A brief discussion of the equation above might be useful. The shift in the Fermi function simply indicates the position of the Fermi level. Due to the proximity of the sample to the active lead, the positive potential on the lead shifts the DOS of the sample downwards (see Fig. 2). This is

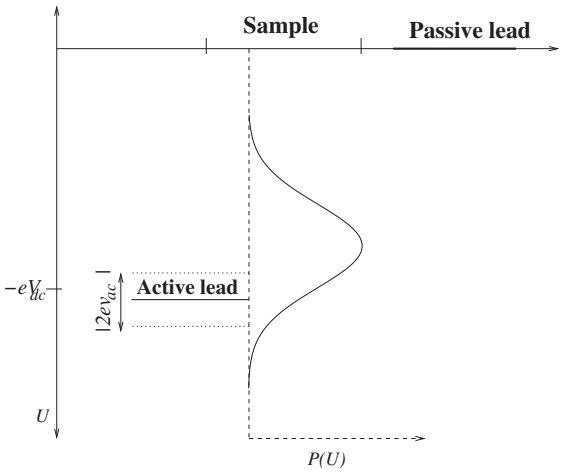

FIG. 2. Energy level diagram at the instant at which charge is calculated. Dark lines depict the Fermi level of the respective leads, dotted line depicts the ac modulation, the curve in the center depicts DOS of the sample under study.

modeled by a coupling capacitor C_a between the sample and the active lead. Since the time scale of tunneling of electrons[28] is much smaller than the time period of the applied ac signal (1 ns–1 ms to suit the capacitance measuring device), the energy level position is assumed to be static for the calculation of charge. As the QD is coupled capacitatively to both the leads, the charge q induces some charge equal to a fraction, say αq, on the active lead. The fraction α depends on the charge on the active lead.

Now, the instantaneous current i through the active lead is obtained by differentiating the charge on it.

$$i = \frac{d(\alpha q)}{dt} = -2e\alpha \int_{-\infty}^{\infty} \left[D\left(E + e\frac{C_a}{C}V\right)\frac{\partial}{\partial t}f(E+eV) + f(E+eV)\frac{\partial}{\partial t}D\left(E + e\frac{C_a}{C}V\right)\right] dE. \tag{6}$$

Since we have already set the resolution of our experiment to poorer than thermal broadening ($v_{ac} > kT$) we are justified in treating the Fermi function $f(E)$ as a unit step function centered at E and hence, its derivative is a δ function. Using Eq. (4) we obtain

$$i = -2e^2\alpha v_{ac}\omega \cos \omega t \left[D\left(e\frac{C_a}{C}V - eV\right) + \frac{C_a}{C}\int_{-\infty}^{-eV} D'\left(E + e\frac{C_a}{C}V\right)dE\right],$$

where the prime stands for the derivative. The second term on the right-hand side of the above equation is simply the DOS at a given energy, in other words, a finite quantity. This term can be ignored since C_a/C is very small (note that $C = C_a + C_p$, with $C_a \ll C_p$). Thus we obtain the current (i),

$$i = -2e^2\alpha v_{ac}\omega D\left(\frac{C_p}{C}U\right)\cos \omega t, \tag{7}$$

where V_{dc} is transformed to energy axis (U) on multiplication by the electronic charge.

Since it is customary to talk in terms of ac capacitance C_{ac} ($\sim i \cos \omega t/\omega v_{ac}$), the equation above is rewritten as

$$C_{ac} = 2e^2\alpha D\left(\frac{C_p}{C}U\right). \tag{8}$$

Hence the ac capacitance of the sample as a function of V_{dc} yields the DOS $[P(U)]$ of the sample under study.

We pause to point out the conditions under which $D(U)$ is directly proportional to $P(U)$. We assume (i) there are a large number of QDs in the sample. (ii) There is no mutual correlation between the QDs, i.e., occupancy of one QD does not affect the probability of occupancy of any other QD. (iii) The capacitative coupling of each QD with the metal lead is the same. The physical significance of the last assumption is that an electron tunneling from the lead to the sample can occupy any QD with equal probability. Further, since $C_p \approx C$,

$$C_{ac} = \gamma 2e^2\alpha P(U), \tag{9}$$

where γ is a proportionality constant.

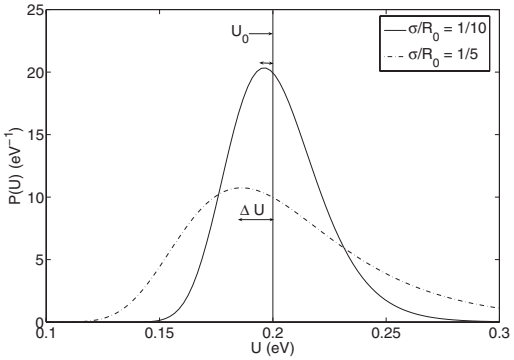

FIG. 3. The distribution $P(U)$ vs U for Gaussian distribution in size. Horizontal arrow indicate the downshift [see Eq. (15)]. The values assumed for the above plot are U_0=0.2 eV, R_0=5 nm, and β=1.

III. UNIMODAL SIZE DISORDER

As stated in the Introduction our aim here is to understand CB for a distribution of QDs. In the following sections we have considered some possible distributions.

A. Gaussian distribution

The growth of the QDs is a stochastic process and it appears reasonable to assume dots with a Gaussian distribution in radius R centered around a mean R_0,

$$P_R = \frac{1}{\sqrt{2\pi}\sigma}\exp\left(-\frac{(R-R_0)^2}{2\sigma^2}\right), \tag{10}$$

$$U_0 = \frac{C}{R_0^\beta}, \tag{11}$$

where we pause to define a mean Hubbard U_0 related to the mean dot radius R_0 [see Eq. (1)].

The CB line shape is determined by transforming Eq. (3) to the energy axis,

$$P(U) = \frac{1}{\sqrt{2\pi}\sigma}\int_0^\infty \delta\left(U - \frac{C}{R^\beta}\right)\exp\left(-\frac{(R-R_0)^2}{2\sigma^2}\right)dR. \tag{12}$$

This is solved to obtain

$$P(U) = \frac{1}{\sigma\sqrt{2\pi}}\frac{C^{1/\beta}}{\beta U^{(1+\beta)/\beta}}\exp\left[-\frac{C^{2/\beta}}{2\sigma^2}\left(\frac{1}{U^{1/\beta}} - \frac{1}{U_0^{1/\beta}}\right)^2\right]. \tag{13}$$

The method above is similar to the one used by Kane for the density of states (DOS) of a disordered system[16] and by John and Singh[17] for the photoluminescence spectra in porous silicon.

The CB line shape is approximately Gaussian for small σ/R_0 as can be seen in Fig. 3. Note that quasisquare well confinement (β=1) has been assumed in plotting the figure. Another aspect worth noting is that the mean Hubbard U_0 and the location of the Hubbard peak (U_p) are not identical.

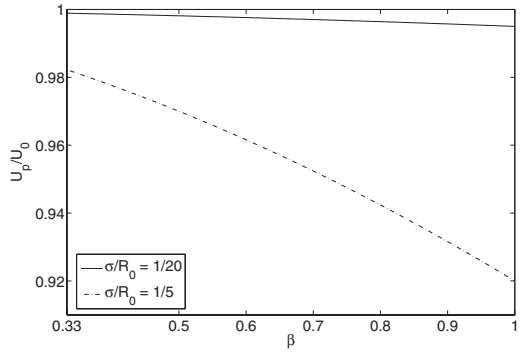

FIG. 4. U_p/U_0 for Gaussian distribution in sizes of QDs. Clearly there is suppression of CB which increases with β and disorder.

To quantify this, we equate the derivative of Eq. (13) to zero and obtain

$$U_p = U_0\left(\frac{-R_0^2/\sigma^2 + \sqrt{R_0^4/\sigma^4 + 4(\beta+1)R_0^2/\sigma^2}}{2(\beta+1)}\right)^{\beta}. \quad (14)$$

For $\sigma/R_0 \to 0$, $U_p = U_0$, as expected. However, for reasonable σ the above expression can be Taylor expanded and neglecting the third and higher order terms, we obtain

$$U_0 - U_p = \Delta U \approx U_0(\beta+\beta^2)\frac{\sigma^2}{R_0^2}. \quad (15)$$

Thus we see a clear downshift. This is indicated in Fig. 3 by the horizontal arrow.

For a better insight we analyze U_p/U_0 with respect to β. This has been depicted in Fig. 4. It can be seen that the ratio decreases with increasing β, i.e., the suppression of CB is more pronounced for quasisquare well confinement as compared to quasiharmonic confinement. Another feature worth noting is that ratio decreases quadratically with σ/R_0, which implies that the suppression becomes more pronounced for greater disorder as expected.

The peak in energy plot is at $P(U_p)$. We can obtain an approximate expression for the full width at half maximum (FWHM) (U_{FWHM}) of the energy profile if the prefactor dependence $U^{(1+\beta)/\beta}$ is ignored. This is calculated for reasonably small σ/R_0 as

$$U_{FWHM} \approx \frac{C}{R_0}\frac{\beta}{R_0^{\beta}}2\sqrt{2\ln 2}\sigma. \quad (16)$$

A larger value of U_{FWHM} is expected if the full expression is employed.

B. Log normal distribution

We now consider log normal distribution in size. For semiconductor nanostructures the log normal size distribution has considerable experimental[19–21] and theoretical support.[22–24] Earlier, Ranjan *et al.* had proposed to reconcile the theory and experiment in case of band gap discrepancies in silicon nanocrystallites using logarithm normal distribution in size.[25]

Here we have

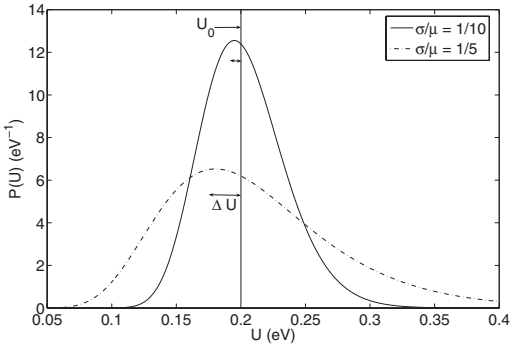

FIG. 5. The distribution $P(U)$ vs U for logarithm normal distribution in size. Horizontal arrow indicate the downshift. The values assumed for the plot above are U_0=0.2 eV, R_0=5 nm, and β=1.

$$P_R = \frac{1}{R\sigma\sqrt{2\pi}}\exp\left(-\frac{(\ln R - \mu)^2}{2\sigma^2}\right). \quad (17)$$

We denote the radius corresponding to the peak in P_R as R_0.

$$R_0 = e^{(\mu-\sigma^2)}. \quad (18)$$

We use Eq. (12) with the Gaussian distribution replaced by the logarithm normal [Eq. (17)] to obtain

$$P(U) = \frac{1}{U(\beta\sigma)\sqrt{2\pi}}\exp\left[-\frac{\{\ln U - (\ln C - \beta\mu)\}^2}{2(\beta\sigma)^2}\right]. \quad (19)$$

This is a logarithm normal distribution in U (Fig. 5). An elementary analysis of the above distribution allows us to obtain its peak,

$$U_p = C\exp[-(\beta\mu + \beta^2\sigma^2)]. \quad (20)$$

Rewriting this equation in terms of U_0 [Eq. (11)] for small σ,

$$U_0 - U_p = \Delta U \approx U_0(\beta+\beta^2)\sigma^2. \quad (21)$$

Once again we see a downshift which increases with σ and β. The plot of U_p/U_0 is qualitatively similar to Fig. 4 and is not depicted.

We obtain the FWHM as

$$U_{FWHM} = 2C\exp(-\beta\mu - \beta^2\sigma^2)\sinh(\beta\sigma\sqrt{2\ln 2}). \quad (22)$$

Replacing $\sinh(\beta\sigma\sqrt{2\ln 2})$ in the above expression by $\beta\sigma\sqrt{2\ln 2}$ for small σ, we see that FWHM is directly proportional to σ (neglecting $\beta^2\sigma^2$ with respect to $\beta\mu$ in exponential).

IV. BIMODAL GAUSSIAN DISTRIBUTION

Bimodal distribution (BD) has been observed in III-V QDs.[26] We investigate the nature of CB for the bimodal case. We model BD as the sum of two Gaussian distributions as follows:

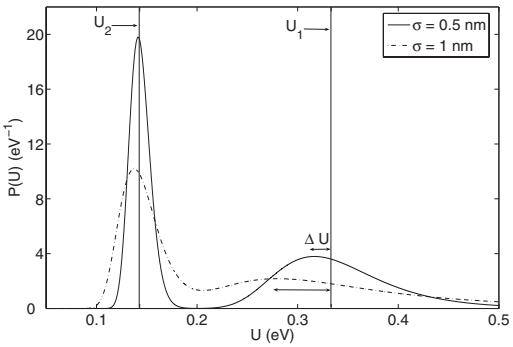

FIG. 6. The distribution $P(U)$ vs U for bimodal distribution in size. Horizontal arrow indicate the downshift. The values assumed for the plot above are U_1=0.33 eV, R_1=3 nm, U_2=0.143 eV, R_2 =7 nm, and β=1.

$$P_R = \frac{1}{2\sigma\sqrt{2\pi}}\left[\exp\left(-\frac{(R-R_1)^2}{2\sigma^2}\right) + \exp\left(-\frac{(R-R_2)^2}{2\sigma^2}\right)\right], \tag{23}$$

where R_1 and R_2 are two radii corresponding to the two peaks with $R_2 > R_1$. Here we have assumed the same σ for both the constituent Gaussian distributions for simplicity. From Eq. (1) we have

$$U_1 = \frac{C}{R_1^\beta}, \quad U_2 = \frac{C}{R_2^\beta}. \tag{24}$$

Transforming Eq. (23) to the energy axis in the usual manner we obtain

$$P(U) = \frac{C^{1/\beta}}{2\beta\sigma\sqrt{2\pi}}\frac{1}{U^{(\beta+1)/\beta}}\left[\exp\left\{-\frac{C^{2/\beta}}{2\sigma^2}\left(\frac{1}{U^{1/\beta}} - \frac{1}{U_1^{1/\beta}}\right)^2\right\} + \exp\left\{-\frac{C^{2/\beta}}{2\sigma^2}\left(\frac{1}{U^{1/\beta}} - \frac{1}{U_2^{1/\beta}}\right)^2\right\}\right]. \tag{25}$$

Figure 6 makes it clear that the distribution obtained above is almost the sum of the individual distributions obtained by transforming the constituent Gaussians to the energy axis. Clearly the two constituent distributions do not interfere with each other as long as $R_2 - R_1 > \sigma$. But as soon as $R_2 - R_1 \approx \sigma$ the two constituent distributions interfere and the locations of the peaks move towards each other. Another feature worth noting is that there is a substantial difference between the heights of the two peaks. This seemingly trivial feature has an important physical consequence.

Assume the QDs to be empty to start with and we start filling electrons, one at a time. We have to add the number of electrons equal to the number of QDs in the assembly. If every QD can take only one electron, then at the end of the distribution of the electrons, all the QDs will have one electron each and CB suppression, though present, will not be consequential. But Hubbard U depends very weakly on the number of electrons in the QD [see Eq. (2)]. Thus the electron will preferentially go to a QD which may already be occupied but at a lower energy and higher $P(U)$ (see Fig. 6). Consequently, a higher number of electrons will be occupying the set of QDs with lower energy and thus CB will be heavily suppressed on average.

Yet another kind of disorder assumes importance in the case of BD. We call it "spatial distribution disorder" (SDD). In the analysis presented above the randomization in the spatial distribution of QDs is neglected altogether. When all the QDs belong to the same size distribution such as in Gaussian and logarithm normal case, the SDD does not play any role. But it assumes importance in the bimodal case when the two constituent Gaussians begin to interfere as the QDs can be thought of as belonging to either of the two (say group "A" and "B").

The situation is analogous to that in a pseudohomogeneous mixture of two metals to form an alloy, which inspired the Lifshitz argument.[15] As argued by Lifshitz, the stochastic clustering of QDs belonging to the same group is bound to alter the behavior of the tails of the DOS [$P(U)$ in this case] of the resulting assembly of QDs. The subject of study here is a two-dimensional spatial distribution of QDs that results in the behavior of $P(U)$ in the tails given by

$$P(U) \simeq \exp\left\{-\left(\frac{c}{U-U_c}\right)\right\}, \tag{26}$$

where c is a positive constant and U_c is the lower or upper energy cutoff depending on which tail of the curve is under consideration. Thus the expression obtained for $P(U)$ has to be altered towards the tails.

V. CONFINEMENT DISORDER

In spite of the most sophisticated experimental techniques, the growth of QDs may lead to irregular charge distribution. This, in turn, gives rise to confinement potentials with considerable disorder. We have also seen [Eq. (1)] that β depends on confinement potential. For the sake of simplicity we model disorder in confinement by a Gaussian distribution in β. Here we assume radius of the QDs to be fairly constant (R) to avoid unnecessary complications. Thus we have

$$P_\beta = \frac{1}{\sigma\sqrt{2\pi}}\exp\left(-\frac{(\beta-\beta_0)^2}{2\sigma^2}\right) \tag{27}$$

and we pause to define U_0 related to mean β_0,

$$U_0 = \frac{C}{(R/R_0)^{\beta_0}}. \tag{28}$$

Here we have taken ratio of R and R_0 to ensure that the denominator is dimensionless. For the remaining analysis we take R_0=1 nm. Transforming Eq. (27) to the energy axis as was done before we obtain

$$P(U) = \frac{1}{U(\sigma \ln R)\sqrt{2\pi}}\exp\left[-\frac{(\ln U - \ln U_0)^2}{2(\sigma \ln R)^2}\right]. \tag{29}$$

This logarithm normal distribution in U is depicted in Fig. 7. Locating the peak of the distribution obtained by the standard method of equating derivative to zero we obtain

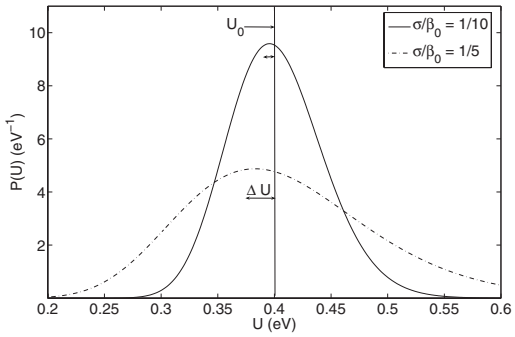

FIG. 7. The distribution $P(U)$ vs U for Gaussian distribution in β. Horizontal arrow indicate the downshift. The values assumed for the plot above are U_0=0.4 eV, R=5 nm, and β_0=0.65.

$$U_0 - U_p = \Delta U = U_0[1 - \exp\{-(\sigma \ln R)^2\}]. \tag{30}$$

For small $\sigma \ln(R)$, which is the case generally, the above expression can be approximated to

$$\Delta U \approx U_0(\sigma \ln R)^2. \tag{31}$$

Once again we see a downshift in U and suppression of CB. To obtain the dependence of downshift on disorder we need to quantify the same. It is reasonable to treat FWHM as the measure of disorder. For small σ, FWHM is calculated to be

$$U_{FWHM} \approx C\frac{\ln R}{R^{\beta_0}}(2\sqrt{2 \ln 2}\sigma). \tag{32}$$

Hence we obtain U_{FWHM} is proportional to σ. Thus, alternately, we can also measure disorder in terms of σ.

VI. DISCUSSION

Coulomb Blockade is suppressed for a disordered assembly of QDs. For both Gaussian and log normal distribution, the suppression is quantified in an approximate way in Eqs. (15) and (21), respectively. The interesting point is that the bimodal distribution suppresses CB even more substantially. Moreover, the Lifshitz argument implies that the spatially disordered distribution alters the behavior of $P(U)$ toward the tails [see Eq. (26)].

Very interestingly, we observe that both types of disorder (size and confinement potential) shift the CB to a lower value. Thus we may expect an attenuation in the CB. We pause to suggest the physical significance of this. There is bound to be a disagreement between theoretically calculated values and experimental values as the former are obtained by usually considering a single QD while experiments are usually carried out on an assembly of QDs. This has been noticed earlier in the context of photoluminescence spectra[17,27] and band gap discrepancies.[25]

Rather fortuitously, analysis of U_{FWHM} with respect to β yields an intriguing result. It can be easily seen that for both the unimodal distributions in sizes, U_{FWHM} as given by Eqs. (16) and (22) has a maximum given by

$$\beta = \frac{1}{\ln R_0}. \tag{33}$$

The result suggests the following. Assuming that the growth of QDs is an equilibrium process, we may argue that resulting assembly has maximum entropy and thus maximum disorder. For a Gaussian or logarithm normal distribution in sizes, the disorder (proportional to U_{FWHM}) is maximized if the above relation holds true. Thus thermodynamic considerations require that β determines the most probable radius R_0. This argument is particularly relevant to self-assembled QDs.

An important remark that must be made is that the model discussed in Sec. II assumes current to be continuous. This is a reasonable assumption for continuous DOS. But if the DOS is composed of discrete energy levels, the sinusoidal nature of the current profile is lost. In such a case, dealing with a single or very few distinct energy levels is easy as the capacitance peaks at these energy levels. Alternatively, when the DOS consists of closely spaced energy levels such that we can have a continuous approximation to the DOS then rectifying the current and measuring its average value should suffice. This gives us DOS irrespective of the current profile. The discrete energy levels case has been studied by a large number of workers already and thus does not merit further discussion.[2]

The work can be extended in a number of ways. Our methodology is not limited to Gaussian or logarithm normal distribution. Any (experimentally verified) distribution can be used. We could use a path integral approach and include some correlation. This would then be similar to work done earlier[29–31] to improve the Kane theory.[16] We could also supplement it by a variational strategy akin to Lloyd and Best variation principle.[32] We believe however that one must first evaluate our theoretical framework using some experimental setup, perhaps the one proposed by us.

ACKNOWLEDGMENTS

This work was supported by the National Initiative on Undergraduate Sciences (NIUS) undertaken by the Homi Bhabha Centre for Science Education—Tata Institute of Fundamental Research (HBCSE-TIFR), Mumbai, India. We thank Mandar Deshmukh of TIFR for valuable discussions.

*praveen@hbcse.tifr.res.in

[1] R. C. Ashoori, H. L. Stormer, J. S. Weiner, L. N. Pfeiffer, S. J. Pearton, K. W. Baldwin, and K. W. West, Phys. Rev. Lett. **68**, 3088 (1992).
[2] R. C. Ashoori, Nature (London) **379**, 413 (1996).
[3] Lei Zhuang, Lingjie Guo, and Stephen Y. Chou, Appl. Phys. Lett. **72**, 1205 (1998).
[4] M. Bayer, O. Stern, P. Hawrylak, S. Fafard, and A. Forchel, Nature (London) **405**, 923 (2000).
[5] T. P. Smith III, K. Y. Lee, C. M. Knoedler, J. M. Hong, and D. P. Kern, Phys. Rev. B **38**, 2172 (1988).
[6] D. Heitmann and J. P. Kotthaus, Phys. Today **46**, 56 (1993).
[7] W. Hansen, T. P. Smith III, K. Y. Lee, J. A. Brum, C. M. Knoedler, J. M. Hong, and D. P. Kern, Phys. Rev. Lett. **62**, 2168 (1989).
[8] B. Meurer, D. Heitmann, and K. Ploog, Phys. Rev. Lett. **68**, 1371 (1992).
[9] R. Pino, A. J. Markvoort, and P. A. J. Hilbers, Eur. Phys. J. B **23**, 103 (2001).
[10] G. Medeiros-Ribeiro, F. G. Pikus, P. M. Petroff, and A. L. Efros, Phys. Rev. B **55**, 1568 (1997).
[11] E. V. Shevchenko, D. V. Talapin, N. A. Kotov, S. O'Brien, and C. B. Murray, Nature (London) **439**, 55 (2006).
[12] M. Tinkham, Am. J. Phys. **64**(3), 343 (1996).
[13] See, for example, V. Ranjan, R. K. Pandey, Manoj K. Harbola, and Vijay A. Singh, Phys. Rev. B **65**, 045311 (2002), and references therein.
[14] R. K. Pandey, Manoj K. Harbola, and Vijay A. Singh, Phys. Rev. B **67**, 075315 (2003).
[15] I. M. Lifshitz, Adv. Phys. **13**, 483 (1964).
[16] E. O. Kane, Phys. Rev. **131**, 79 (1963).
[17] George C. John and Vijay A. Singh, Phys. Rev. B **50**, 5329 (1994).
[18] K. H. Schmidt, G. Medeiros-Ribeiro, and P. M. Petroff, Phys. Rev. B **58**, 3597 (1998).
[19] T. van Buuren, L. N. Dinh, L. L. Chase, W. J. Siekhaus, and L. J. Terminello, Phys. Rev. Lett. **80**, 3803 (1998).
[20] Yoshihiko Kanemitsu, Tetsuo Ogawa, Kenji Shiraishi, and Kyozaburo Takeda, Phys. Rev. B **48**, 4883 (1993).
[21] Qi Zhang, S. C. Bayliss, and D. A. Hutt, Appl. Phys. Lett. **66**, 1977 (1995).
[22] Manish Kapoor and Vijay A. Singh, Mod. Phys. Lett. B **13**, 703 (1999).
[23] H. Yorikawa and S. Muramatsu, Appl. Phys. Lett. **71**, 644 (1997).
[24] S. Datta and K. L. Narasimhan, Phys. Rev. B **60**, 8246 (1999).
[25] V. Ranjan, Manish Kapoor, and Vijay A. Singh, J. Phys.: Condens. Matter **14**, 6647 (2002).
[26] B. Bansal, M. R. Gokhale, A. Bhattacharya, and B. M. Arora, Appl. Phys. Lett. **87**, 203104 (2005).
[27] O. K. Andersen and E. Veje, Phys. Rev. B **53**, 15643 (1996).
[28] Khairurrijal, Fatimah A. Noor, and Sukirno, Solid-State Electron. **49**, 923 (2005).
[29] B. I. Halperin and M. Lax, Phys. Rev. **148**, 722 (1966).
[30] S. F. Edwards, J. Phys. C **3**, L30 (1970).
[31] V. Samathiyakanit, J. Phys. C **7**, 2849 (1974).
[32] P. Lloyd and P. R. Best, J. Phys. C **8**, 3752 (1975).